Supporting Information

For

Metal atom lability in polynuclear complexes

Emily V. Eames, Raul Hernández-Sánchez, and Theodore A. Betley*

Department of Chemistry and Chemical Biology, Harvard University
12 Oxford Street, Cambridge MA 02138

Experimental Section

Materials and Methods. All manipulations involving metal complexes were carried out using standard Schlenk line or glove-box techniques under a dinitrogen atmosphere. All glassware was oven-dried for a minimum of 4 h and cooled in an evacuated antechamber prior to use in the dry box. Benzene, diethyl ether, acetonitrile ($NCCH_3$) and tetrahydrofuran (THF) were dried and deoxygenated on a Glass Contour System (SG Water USA, Nashua, NH) and stored over 4 Å molecular sieves (Strem) prior to use. Benzene-d_6, $NCCH_3$-d_3 and THF-d_8 were purchased from Cambridge Isotope Labs and were degassed and stored over 4 Å molecular sieves prior to use. Solvents were typically tested with a standard purple solution of sodium benzophenone ketyl in THF in order to confirm effective oxygen and moisture removal. $MeC(CH_2NHPh\text{-}o\text{-}NHPh)_3$ (^{Ph}L), [1] (^{Ph}L)$Fe_3(thf)_3$ and [(^{Ph}L)$Fe_3(\mu\text{-}Cl)]_2$ (**1**)[2] were prepared following published methods. ^{57}Fe powder was purchased from Cambridge Isotope Labs and converted to ^{57}Fe-enriched $FeCl_2$ by conproportionation with $FeCl_3$ following the procedure outlined by Wilkinson.[3] All other reagents were purchased from commercial vendors and used without further purification unless explicitly stated.

Physical Measurements. All of the measurements for the metal complexes except XRF analysis were made under anaerobic conditions. Elemental analyses were performed by Complete Analysis Laboratories, Inc., Parsippany, New Jersey. ^1H NMR spectra were recorded on a Varian Unity/Inova 500B NMR spectrometer with chemical shifts (δ ppm) referenced to residual NMR solvent. UV/Visible spectra were recorded on a Varian Cary 50 UV/Visible spectrometer using quartz cuvettes. NIR spectra were recorded on a PerkinElmer Lambda 750 high-performance UV-vis spectrometer.

X-ray fluorescence analyses were recorded on a Bruker Tracer III-SD XRF analyzer with the yellow filter (composition 12 mil Al and 1 mil Ti, passes 12-40 keV) and data was collected on each sample for at least 2 min. Samples for the calibration curve were prepared by grinding together cobalt(II)chloride hexahydrate and ferrous chloride tetrahydrate. The spectra of pure Fe and Co were each fit to two Voigt lineshapes. The calibration samples were then fit to four Voigt lineshapes, with the areas of each peak varying freely but all other parameters held to the reference values. Fits are substantially poorer if the Kα:Kβ peak area ratios are fixed, though the overall results are unchanged. Quantification was performed using only the Kα peak areas, but there is no difference in result if the Kα and Kβ areas are summed. Fe:Co ratios in samples were determined by fitting using the calibration data and calculating the Fe:Co ratio from the peak area ratios using the linear fit to the calibration curve.

Magnetic measurements were recorded using a Quantum Design MPMS-XL magnetometer. Powdered samples were placed in Lilly #4 gel capsules and thoroughly saturated with melted eicosane wax to prevent particle torquing in the magnetic field. Samples were suspended in the magnetometer using plastic straws. Samples were prepared under dinitrogen atmosphere in a glovebox. Dc magnetic susceptibility data were collected in the temperature range 5-300 K under fields of 0.1, 0.5, 1 and 2 T. Magnetization data were acquired at 1.8-10 K under fields of 1, 2, 3, 4, 5, 6, and 7 T. Susceptibility data were corrected for the diamagnetic contribution of a blank sample consisting of the wax, capsule and straw at the correct field and temperature. The magnetic susceptibilities were adjusted for diamagnetic contributions using the constitutive corrections from Pascal's constants. The molar magnetic susceptibility (χ_m)

was calculated by converting the magnetization (M) obtained from the magnetometer to a molar susceptibility using the multiplication factor [molecular weight (MW)]/[sample weight (m) × field strength (H)]. All samples were checked for ferromagnetic impurities by collecting a field dependence curve at 100 K and samples were rejected if any deviation from linearity was observed.

Zero-field, ^{57}Fe Mössbauer spectra were measured on a constant acceleration spectrometer (SEE Co, Minneapolis, MN) with a Janis SVT-100 cryostat. Isomer shifts are quoted relative to α-Fe foil (< 25 μm thick) at room temperature. Samples were prepared using approximately 30 mg of sample suspended in paratone-N oil. Temperatures were controlled using a LakeShore 321 autotuning temperature controller. Temperature variations were no greater than ±10 K, and were generally within ±2 K. Data were analyzed using an in-house package written by E. R. King and modified by E. V. Eames in Igor Pro (Wavemetrics).

Preparation of (^{Ph}L)$_2$Fe$_7$(μ-Cl)$_4$(thf)$_2$ (2). A chilled (–35 °C) solution of [(^{Ph}L)Fe$_3$(μ-Cl)]$_2$ (**1**) (100 mg, 61.3 μmol, 1 equiv) in tetrahydrofuran (15 mL) was added to solid $FeCl_2$ (8 mg, 63.5 μmol, 1.04 equiv) and stirred for 3 h, allowing the reaction to warm to room temperature. The volatiles were removed under vacuum. Benzene (5 mL) was added with three drops of tetrahydrofuran to the solids and the resulting solution was filtered through a pipette fitted with filter paper and stored at room temperature. The resulting precipitate was washed with diethyl ether and dried under vacuum. Yield: 60 mg (52%). X-ray quality crystals were grown from a concentrated solution in benzene at

room temperature. Anal. Calcd for $C_{90}H_{88}Fe_7N_{12}Cl_4O_2$: C 56.82, H 4.66, N 8.83. Found: C 56.57, H 4.61, N 8.71.

Preparation of (^{Ph}L)$_2$Fe$_6$Co(μ-Cl)$_4$(thf)$_2$ (3). A chilled (–35 °C) solution of **1** (60 mg, 37 μmol, 1 equiv) in tetrahydrofuran (15 mL) was added to solid $CoCl_2$ (4.8 mg, 37 μmol, 1 equiv) and stirred for 3 h, allowing the reaction to warm to room temperature. The volatiles were removed under vacuum. Benzene (5 mL) was added with three drops of tetrahydrofuran to the solids and the resulting solution was filtered through a pipette fitted with filter paper and stored at room temperature. The resulting precipitate was washed with benzene and dried under vacuum. Yield: 35 mg (51%). X-ray quality crystals were grown from a concentrated solution in benzene at room temperature. Anal. Calcd for $C_{90}H_{88}Fe_6CoN_{12}Cl_4O_2$: C 56.73, H 4.65, N 8.82. Found: C 56.69, H 4.58, N 8.75.

Preparation of (^{Ph}L)Fe$_2$CoCl(NCCH$_3$) (4). A solution of **1** (130 mg, 80 μmol, 1 equiv) in thawing tetrahydrofuran (20 mL) was added to solid $CoCl_2$ (21.2 mg, 164 μmol, 2.06 equiv) and stirred for 3 h, allowing the reaction to warm to room temperature. The volatiles were removed under vacuum. Acetonitrile (2 mL) was added, briefly dissolving the solid and rapidly precipitating a crystalline product. The crystals were collected on a fritted glass funnel and washed with acetonitrile (3 mL), then dissolved in benzene and filtered to remove any insoluble material. The volatiles were removed under vacuum, and 4 drops of tetrahydrofuran were added, followed by acetonitrile (2 mL). The product, which precipitated from acetonitrile, was collected on a fritted glass funnel and washed with more acetonitrile, then dried under vacuum. Recrystallized yield: 58 mg (42%). X-ray quality crystals were grown from a concentrated solution in acetonitrile at room

temperature. ^{1}H NMR (C_6D_6 with 3 drops $NCCH_3$-d_3, 500 MHz, δ, ppm): 54, 48, 46, 45, 41, 23, 17, 16, 11, 5, 2, -2, -5, -14, -29, -39, -72, -77, -90. Anal. Calcd for $C_{43}H_{39}Fe_2CoN_7Cl$: C 60.06, H 4.57, N 11.40. Found: C 59.96, H 4.59, N 11.42.

Preparation of (^{Ph}L)FeCo$_2$Cl(NCCH$_3$) (5). A solution of **1** (140 mg, 86 μmol, 1 equiv) in thawing tetrahydrofuran (20 mL) was added to solid $CoCl_2$ (57.1 mg, 443 μmol, 5.1 equiv) and stirred for 3 h, allowing the reaction to warm to room temperature. The volatiles were removed under vacuum. Acetonitrile (2 mL) was added, briefly dissolving the solid and rapidly precipitating a crystalline product. The crystals were collected on a fritted glass funnel and washed with acetonitrile (3 mL), then dissolved in benzene and filtered to remove any insoluble material. The volatiles were removed under vacuum, and 4 drops of tetrahydrofuran were added, followed by acetonitrile (2 mL). The product, which precipitated from acetonitrile, was collected on a fritted glass funnel and washed with more acetonitrile, then dried under vacuum. Recrystallized yield: 60.3 mg (41%). X-ray quality crystals were grown from a concentrated filtered solution in acetonitrile at room temperature. ^{1}H NMR (C_6D_6 with 3 drops $NCCH_3$-d_3, 500 MHz, δ, ppm): 48, 46, 30, 28, 26, 24, 17, 15, 11, 10, 5.5, -2, -4, -8, -16, -19, -29, -39, -42, -56, -72. Anal. Calcd for $C_{43}H_{39}FeCo_2N_7Cl$: C 59.85, H 4.55, N 11.36. Found: C 59.75, H 4.66, N 11.28.

Preparation of [(^{Ph}L)FeCo$_2$(μ-Cl)]$_2$ (6). A solution of **1** (140 mg, 86 μmol, 1 equiv) in thawing tetrahydrofuran (20 mL) was added to solid $CoCl_2$ (57.1 mg, 443 μmol, 5.1 equiv) and stirred for 5 h, allowing the reaction to warm to room temperature. The volatiles were removed under vacuum. Acetonitrile (2 mL) was added, briefly dissolving the solid and rapidly precipitated a crystalline product. The crystals were collected on a fritted glass funnel and washed with acetonitrile (3 mL), then dissolved in benzene and

filtered to remove any insoluble material. The volatiles were removed under vacuum, followed by dissolution in benzene (5 mL) and the solution stored overnight. The crystalline material was collected on a fritted glass funnel and washed with benzene, then dried under vacuum. Recrystallized yield: 52 mg (37%). X-ray quality crystals were grown from a concentrated solution in benzene at room temperature. Anal. Calcd for $C_{41}H_{36}FeCo_2N_6Cl$: C 59.91, H 4.41, N 10.22. Found: C 59.94, H 4.47, N 10.08.

Preparation of (^{Ph}L)Fe$_3$Cl(NCCH$_3$) (7). To a solution of **1** (50 mg, 31 μmol) in benzene (5 mL) was added 25 drops of acetonitrile. The solution was filtered and the volatiles removed under vacuum. No crystals of this material were ever obtained, despite numerous attempts. Yield: 51 mg (97%). ^{1}H NMR (C_6D_6 with 3 drops $NCCH_3$-*d*$_3$, 500 MHz, δ, ppm): 53, 36, 33, 28, 19, 13.5, 12, 6, -16, -47, -80, -98. Anal. Calcd for $C_{43}H_{39}Fe_3N_7Cl$: C 60.28, H 4.59, N 11.44. Found: C 60.26, H 4.54, N 11.42.

^{57}Fe Exchange Experiments. Degenerative exchange of ^{57}Fe-enriched $FeCl_2(thf)_2$ was observed by zero-field, ^{57}Fe Mössbauer spectroscopy. Enriched $FeCl_2(thf)_2$ (2.5 mg, 0.5 equiv) was dissolved in tetrahydrofuran (2 mL) with stirring, cooled to –35˚C in the glovebox freezer, and added to **1** (30 mg, 18.4 μmol) frozen in 5 mL of tetrahydrofuran. This experiment was performed in triplicate, and the resulting solutions were filtered through a pipette fitted with filter paper and evacuated to dryness (with constant stirring) under vacuum after 0, 2 and 15 h had elapsed. Mössbauer samples were prepared from the collected solids (~15 mg).

X-ray Structure Determinations. A single crystal suitable for X-ray analysis was mounted and centered on the tip of a cryoloop attached to a goniometer head. Cell parameters were determined using the program SMART.[4] Data reduction and integration were performed with the software package SAINT,[5] while absorption corrections were applied using the program SADABS.[6] Space groups were assigned unambiguously by analysis of symmetry, and systematic absences were determined by XPREP. The positions of the heavy atoms were found via direct methods using the program SHELXTL.[7] Subsequent cycles of least-squares refinement followed by difference Fourier syntheses revealed the positions of the remaining non-hydrogen atoms. Hydrogen atoms were added in idealized positions. Non-hydrogen atoms were refined with anisotropic displacement parameters. In disordered structures, phenyl rings were constrained to idealized geometries and anisotropic displacement parameters were restrained as necessary. Crystallographic data are given in Tables S1-2 and selected bond distances and angles in Tables S3-7.

Modeling of Magnetic Data. The susceptibility and reduced magnetization data were modeled using the package MAGPACK.[8] Simulations were run by canvassing a range of parameter values rather than using a fitting algorithm, due to the computational intensity of the calculations. The spin state values reported are the only ones that produced plausible fits, but the exchange, anisotropy and *g* parameters reported should not be taken as definitive, as wide ranges of values gave fits of similar quality. (Anisotropy parameters are not in general reliably determined by fitting magnetic data.) In some cases several plots are shown to demonstrate this (see Figures S20-22). As described in the text each

trinuclear unit was modeled as a high-spin ferrous unit coupled to the M_2^{5+} pair (S = 1, $FeCo^{5+}$; S = 1/2, Co_2^{5+}). Where possible, parameter values were chosen to simultaneously optimize the fit to the reduced magnetization and susceptibility data, but no attempt was made to optimize the combined fit in a rigorously quantitative way.

(1) Eames, E. V.; Harris, T. D.; Betley, T. A. *Chem. Sci.*, **2012**, *3*, 407.
(2) Eames, E. V.; Betley, T. A. *Submitted*.
(3) Wilkinson, G. *Org. Synth.* **1956**, *36*, 31.
(4) SMART V 5.05 Software for the CCD Detector System; Bruker Analytical X-ray System, Inc.: Madison, WI, 1998.
(5) SAINT. Data Reduction Software. V 6.36A; Bruker Analytical X-ray System, Inc.: Madison, WI, 2002.
(6) SADABS. Bruker/Siemens Area Detector Absorption and Other Corrections. V2.03; Bruker Analytical X-ray System, Inc.: Madison, WI, 2002.
(7) Sheldrick, G. M., *SHELXTL. V 6.12*; Bruker Analytical X-ray Systems, Inc.: Madison, WI, 2000.
(8) Borrás-Almenar, J. J.; Clemente-Juan, J. M.; Coronado, A.; Tsukerblat, B. S. *J. Comput. Chem.*, **2001**, *22*, 985.

Figure S1. UV-vis spectra of **1** (red), **4** (green), **5** (blue). All samples were prepared with a stock solution of 2.5% acetonitrile in benzene (wt/wt). Near IR studies reveal no additional bands between 1000-2400 nm.

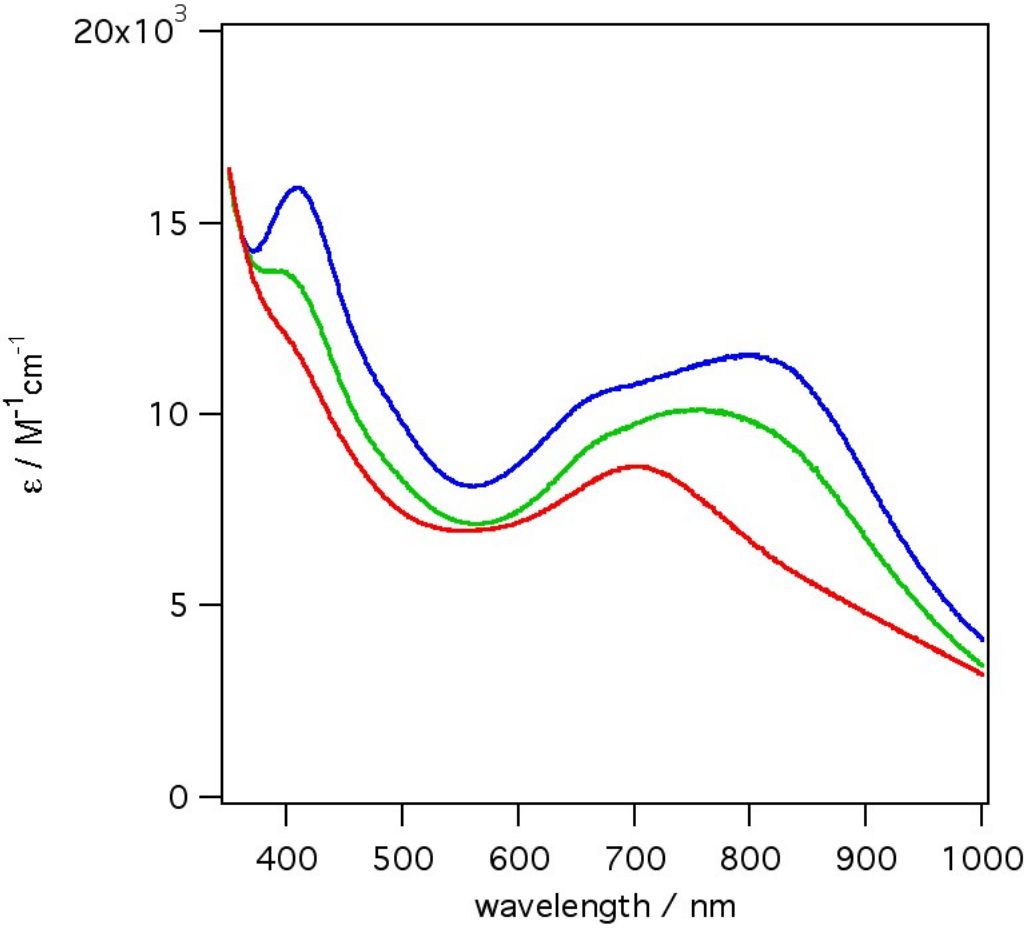

Table S1. X-ray Crystallographic Data for **2-6**.

Complex	**2**	**3**	**4**	**5**	**6**
Chemical formula	$C_{90}H_{88}Fe_7N_{12}Cl_4O_2 \cdot 1.25\ (C_6H_6)$	$C_{90}H_{88}Fe_6CoN_{12}Cl_4O_2 \cdot 1.25\ (C_6H_6)$	$C_{43}H_{39}Fe_2CoN_7Cl \cdot 1.5\ (C_2H_3N)$	$C_{43}H_{39}FeCo_2N_7Cl \cdot 1.5\ (C_2H_3N)$	$C_{82}H_{72}Fe_2Co_4N_{12}Cl_2 \cdot 9.5\ (C_6H_6)$
FW	2171.95	2175.03	1842.95	1849.11	2385.86
Space group	$P\bar{1}$	$P\bar{1}$	$P\bar{1}$	$P\bar{1}$	$P\bar{1}$
a (Å)	12.761(3)	12.761(3)	12.7540(12)	11.1826(10)	18.0835(10)
b (Å)	13.232(3)	13.232(3)	18.1556(16)	11.8436(11)	19.0729(10)
c (Å)	15.826(4)	15.826(4)	19.2333(17)	17.5880(16)	19.3294(10)
α (deg)	79.669(5)	79.669(5)	72.2376(14)	73.4180(10)	74.2878(9)
β (deg)	74.646(5)	74.646(5)	86.4885(14)	82.2320(10)	67.1492(9)
γ (deg)	79.387(5)	79.387(5)	76.0497(14)	67.0980(10)	80.5020(9)
V (Å^3)	2508.9(10)	2508.9(10)	4115.8(6)	2055.8(3)	5900.6(5)
Z	1	1	2	1	2
d_{calcd} (g·cm^{-3})	1.438	1.440	1.487	1.494	1.343
μ (mm^{-1})	1.147	1.168	1.204	1.256	0.891
T (K)	100(2)	100(2)	100(2)	100(2)	100(2)
R1[a]	0.0698	0.0709	0.0413	0.0411	0.1010
wR2[b]	0.1983	0.1588	0.1007	0.0948	0.2914

[a] $R1 = [\sum w(F_o - F_c)^2/\sum wF_o^2]^{1/2}$.

[b] $wR2 = [\sum [w(F_o^2 - F_c^2)^2]/ \sum w(F_o^2)^2]^{1/2}$, $w = 1/[\sigma^2(F_o^2) + (aP)^2 + bP]$, where $P = [\max(F_o^2,0) + 2(F_c^2)]/3$.

Table S2. Selected Core Bond Distances (Å) of **1**-**6**.

	1	**2**	**3**	**4**	**5**	**6**
M(1)–M(2)	2.5889(5)	2.5103(14)	2.5068(17)	2.5427(6) 2.5342(6)	2.5253(6)	2.5101(13)
M(1)–M(3)	2.5801(5)	2.6439(14)	2.5754 (17)	2.5530(6) 2.5221(6)	2.5348(6)	2.5294(14)
M(2)–M(3)	2.3410(5)	2.3177(13)	2.2903(16)	2.2948(6) 2.3013(6)	2.2971(5)	2.2842(13)
M(1)–X	2.3573(6)	2.3246(19)	2.334(2)	2.2413(9) 2.2378(9)	2.2348(9)	2.346(2)
M(1)–L	2.4425(6)	2.403(2)	2.413(2)	2.137(3) 2.125(3)	2.129(3)	2.438(2)
M(1)–N(2)	2.081(2)	2.107(5)	2.069(6)	2.066(2) 2.091(2)	2.068(2)	2.071(6)
M(1)–N(3)	2.092(2)	2.121(5)	2.133(6)	2.085(2) 2.072(2)	2.088(2)	2.084(6)
M(2)–N(1)	1.923(2)	1.979(5)	1.940(6)	1.927(2) 1.948(2)	1.925(2)	1.934(6)
M(2)–N(3)	1.9266(19)	1.912(6)	1.945(7)	1.919(2) 1.913(2)	1.919(2)	1.913(6)
M(2)–N(4)	1.978(2)	2.069(6)	2.029(7)	2.003(2) 2.034(2)	2.001(2)	2.024(6)
M(2)–N(6)	1.8552(19)	1.886(5)	1.843(6)	1.853(2) 1.869(2)	1.855(2)	1.846(6)
M(3)–N(1)	1.965(2)	1.918(5)	1.907(6)	1.955(2) 1.924(2)	1.950(2)	1.901(6)
M(3)–N(2)	1.916(2)	1.932(5)	1.925(6)	1.914(2) 1.926(2)	1.910(2)	1.934(6)
M(3)–N(4)	2.059(2)	1.977(5)	1.979(7)	2.027(2) 2.006(2)	2.025(2)	2.011(6)
M(3)–N(5)	1.872(2)	1.847(5)	1.835(6)	1.861(2) 1.854(2)	1.865(2)	1.840(6)

Table S3. Selected Ligand Bond Distances (Å) for **2**.

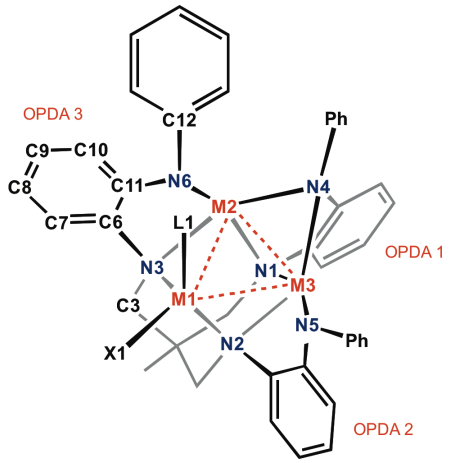

OPDA subunit	**1**	**2**	**3**
C(3)–N(1)	1.463(8)	1.464(8)	1.482(8)
N(1)–C(6)	1.415(8)	1.411(8)	1.430(8)
C(6)–C(7)	1.384(9)	1.373(9)	1.395(10)
C(7)–C(8)	1.397(10)	1.398(9)	1.410(10)
C(8)–C(9)	1.357(9)	1.368(10)	1.386(11)
C(9)–C(10)	1.408(9)	1.391(9)	1.395(11)
C(10)–C(11)	1.377(9)	1.398(9)	1.404(10)
C(6)–C(11)	1.407(9)	1.406(9)	1.403(10)
C(11)–N(4)	1.441(8)	1.380(8)	1.376(9)
N(4)–C(12)	1.419(8)	1.416(8)	1.446(10)

Table S4. Selected Ligand Bond Distances (Å) for **3**.

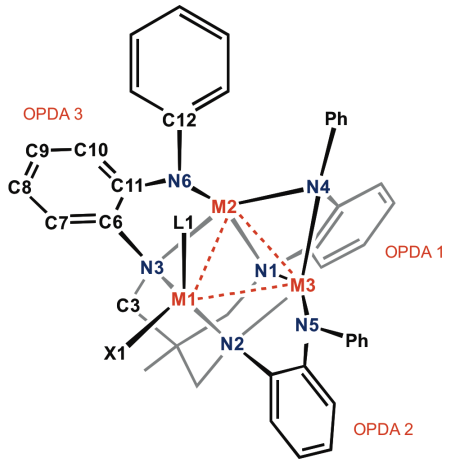

OPDA subunit	**1**	**2**	**3**
C(3)–N(1)	1.484(9)	1.477(9)	1.463(9)
N(1)–C(6)	1.425(9)	1.402(9)	1.399(9)
C(6)–C(7)	1.381(10)	1.382(10)	1.396(11)
C(7)–C(8)	1.391(11)	1.393(10)	1.388(11)
C(8)–C(9)	1.387(11)	1.379(11)	1.416(12)
C(9)–C(10)	1.385(10)	1.376(10)	1.387(12)
C(10)–C(11)	1.383(10)	1.396(10)	1.423(11)
C(6)–C(11)	1.437(10)	1.425(11)	1.386(11)
C(11)–N(4)	1.444(9)	1.370(9)	1.404(10)
N(4)–C(12)	1.442(9)	1.423(9)	1.428(11)

Table S5. Selected Ligand Bond Distances (Å) for **4**.

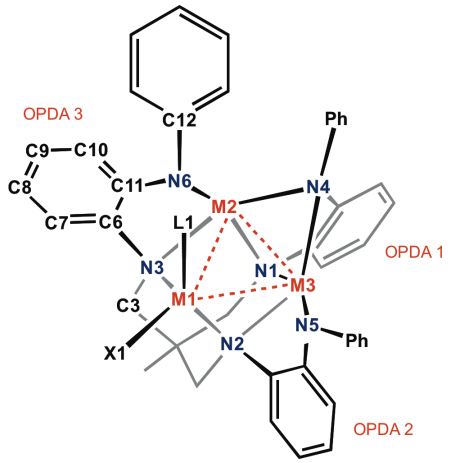

OPDA subunit	**1**	**2**	**3**
C(3)–N(1)	1.460(3)	1.492(3)	1.478(3)
N(1)–C(6)	1.423(4)	1.433(4)	1.415(4)
C(6)–C(7)	1.378(4)	1.385(4)	1.395(4)
C(7)–C(8)	1.398(4)	1.389(4)	1.382(4)
C(8)–C(9)	1.386(4)	1.395(4)	1.390(4)
C(9)–C(10)	1.391(4)	1.379(4)	1.388(4)
C(10)–C(11)	1.387(4)	1.408(4)	1.400(4)
C(6)–C(11)	1.414(4)	1.416(4)	1.412(4)
C(11)–N(4)	1.430(4)	1.385(4)	1.394(4)
N(4)–C(12)	1.436(3)	1.416(3)	1.433(4)

Table S6. Selected Ligand Bond Distances (Å) for **5**.

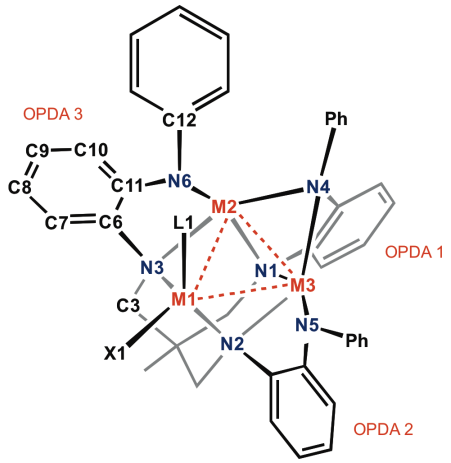

OPDA subunit	**1**	**2**	**3**
C(3)–N(1)	1.461(3)	1.490(3)	1.473(4)
N(1)–C(6)	1.422(3)	1.429(3)	1.418(3)
C(6)–C(7)	1.384(4)	1.382(4)	1.398(4)
C(7)–C(8)	1.387(4)	1.388(4)	1.385(4)
C(8)–C(9)	1.385(4)	1.393(4)	1.380(6)
C(9)–C(10)	1.400(4)	1.375(4)	1.396(5)
C(10)–C(11)	1.385(4)	1.408(4)	1.406(4)
C(6)–C(11)	1.408(4)	1.420(4)	1.406(5)
C(11)–N(4)	1.431(3)	1.384(4)	1.390(4)
N(4)–C(12)	1.434(3)	1.420(3)	1.433(4)

Table S7. Selected Ligand Bond Distances (Å) for **6**.

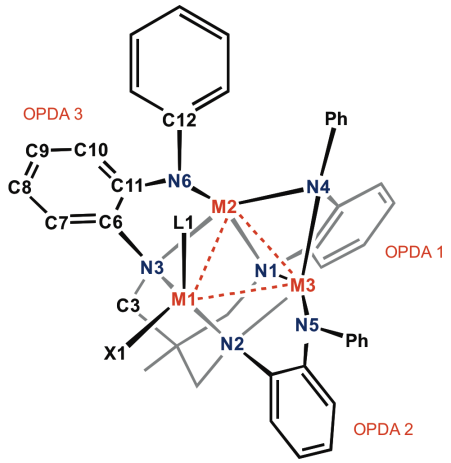

OPDA subunit	**1**	**2**	**3**
C(3)–N(1)	1.455(10)	1.468(10)	1.488(9)
N(1)–C(6)	1.422(10)	1.426(9)	1.425(9)
C(6)–C(7)	1.388(11)	1.396(10)	1.383(11)
C(7)–C(8)	1.411(12)	1.411(11)	1.398(11)
C(8)–C(9)	1.351(14)	1.387(13)	1.389(12)
C(9)–C(10)	1.403(12)	1.382(12)	1.379(11)
C(10)–C(11)	1.392(12)	1.416(10)	1.407(10)
C(6)–C(11)	1.396(12)	1.386(11)	1.400(10)
C(11)–N(4)	1.435(10)	1.387(9)	1.402(9)
N(4)–C(12)	1.410(10)	1.429(11)	1.426(9)

Figure S2. Solid state structure of **2** with the thermal ellipsoids set at the 30% probability level (hydrogen atoms and solvent molecules omitted for clarity; only one site shown for disordered atoms; Fe orange, C black, N blue, Cl green).

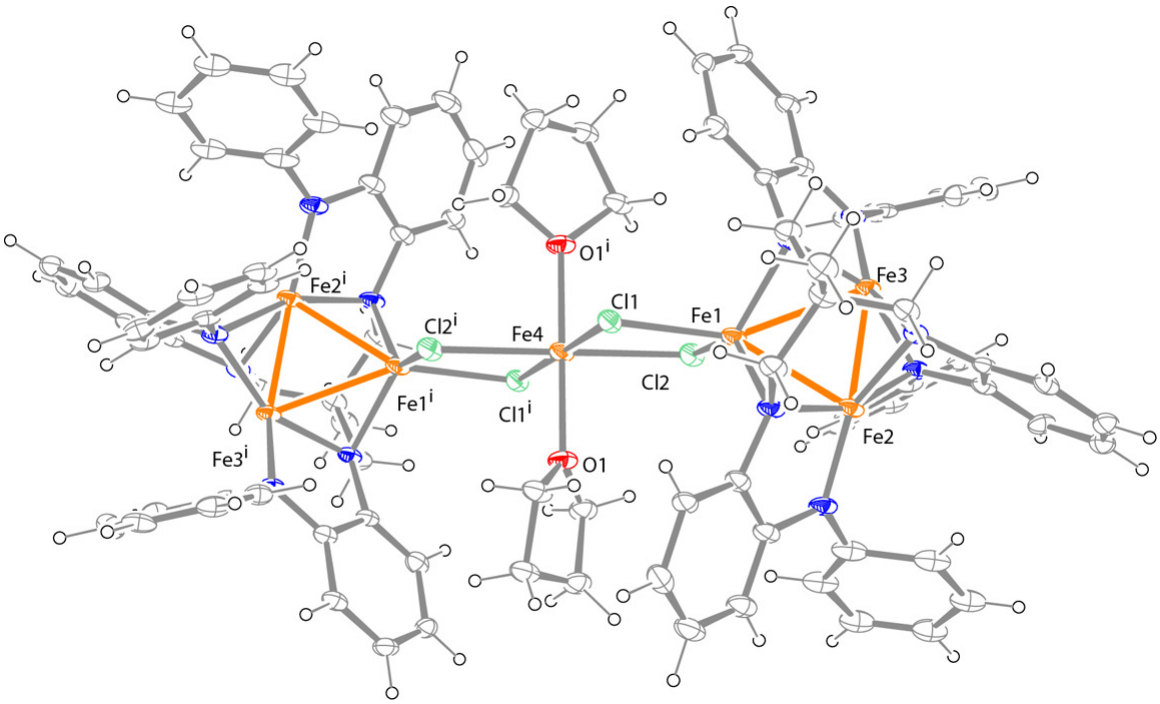

Figure S3. Solid state structure of **3** the thermal ellipsoids set at the 30% probability level (hydrogen atoms and solvent molecules omitted for clarity; Fe orange, C black, N blue, Cl green, M refers to mixture of Co/Fe).

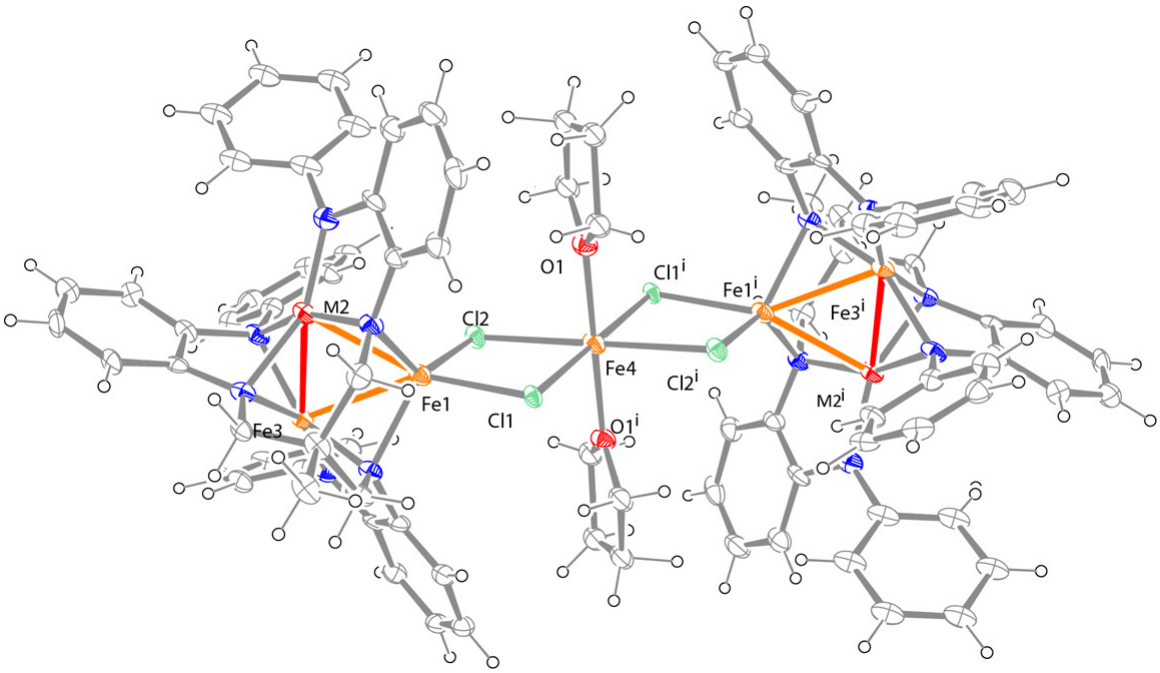

Figure S4. Solid state structure of **4** with the thermal ellipsoids set at the 50% probability level (hydrogen atoms and solvent molecules omitted for clarity; Fe orange, C black, N blue, Br maroon, O red).

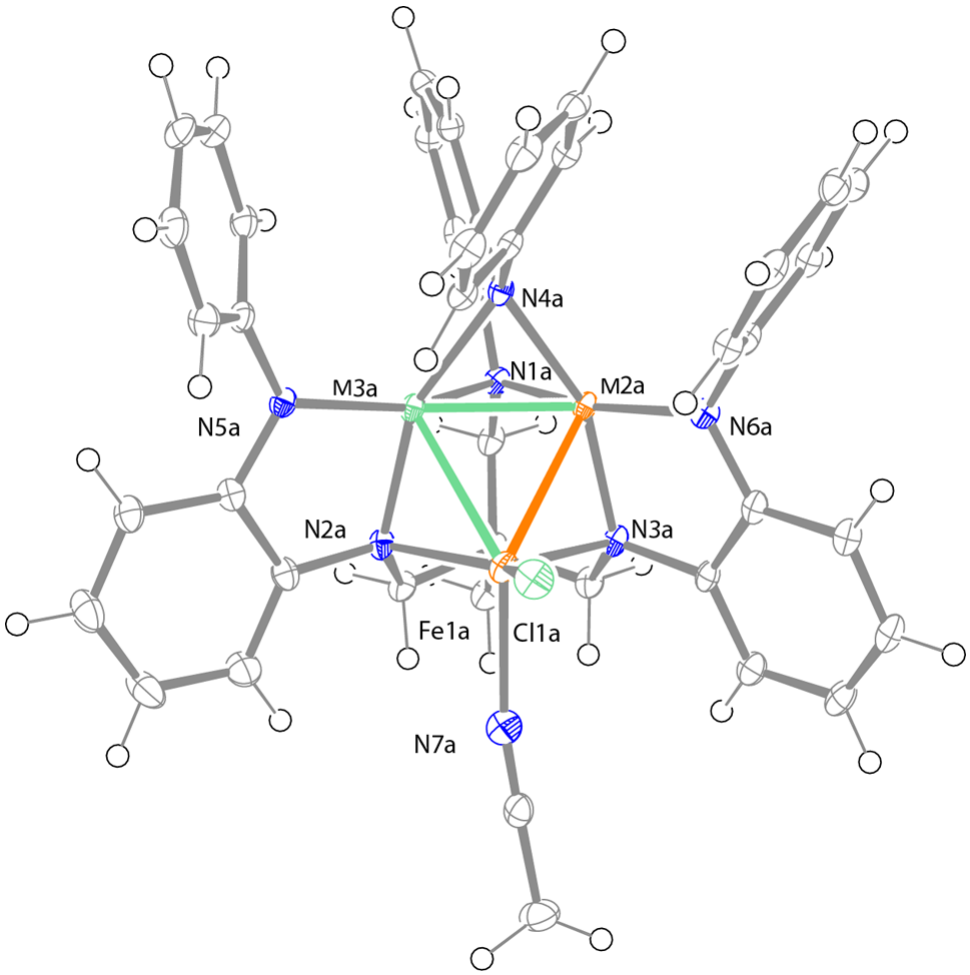

Figure S5. Solid state structure of **5** with the thermal ellipsoids set at the 50% probability level (hydrogen atoms and solvent molecules omitted for clarity; Fe orange, C black, N blue, Br maroon).

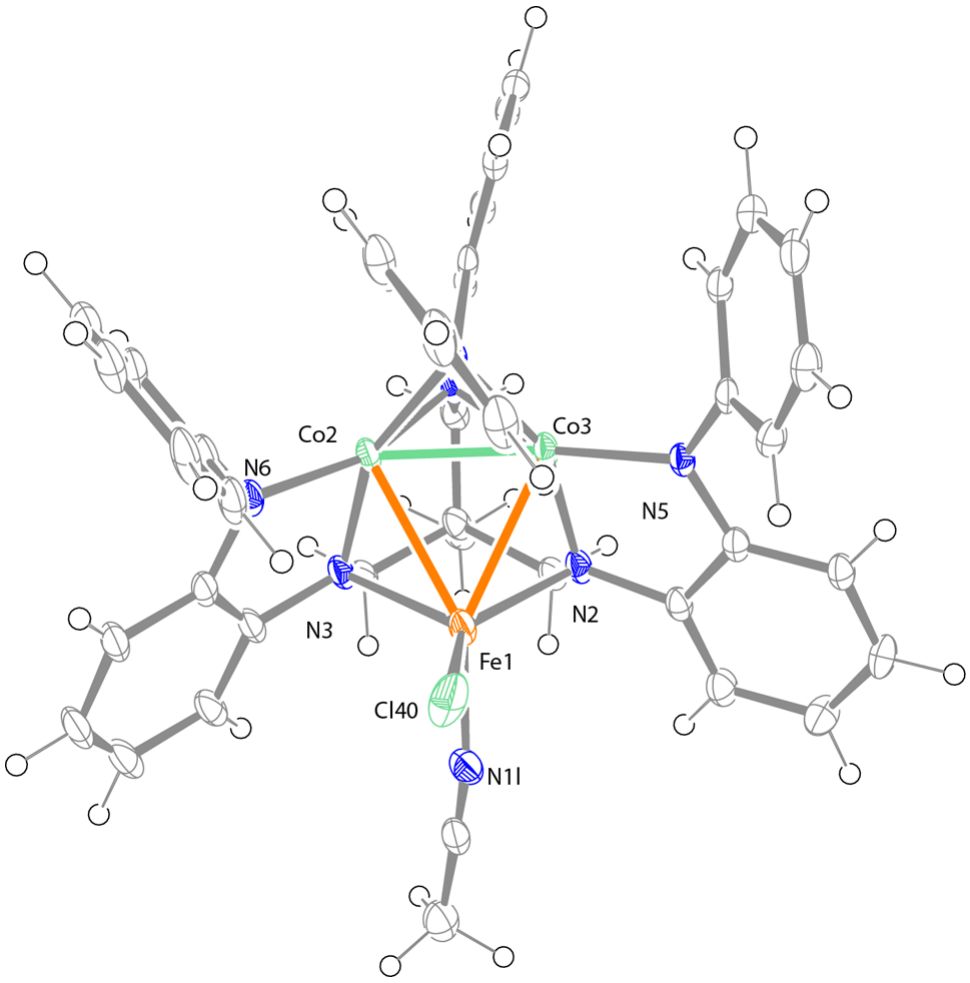

Figure S6. Solid state structure of **6** with the thermal ellipsoids set at the 50% probability level (hydrogen atoms and solvent molecules omitted for clarity; Fe orange, C black, N blue, I green, O red).

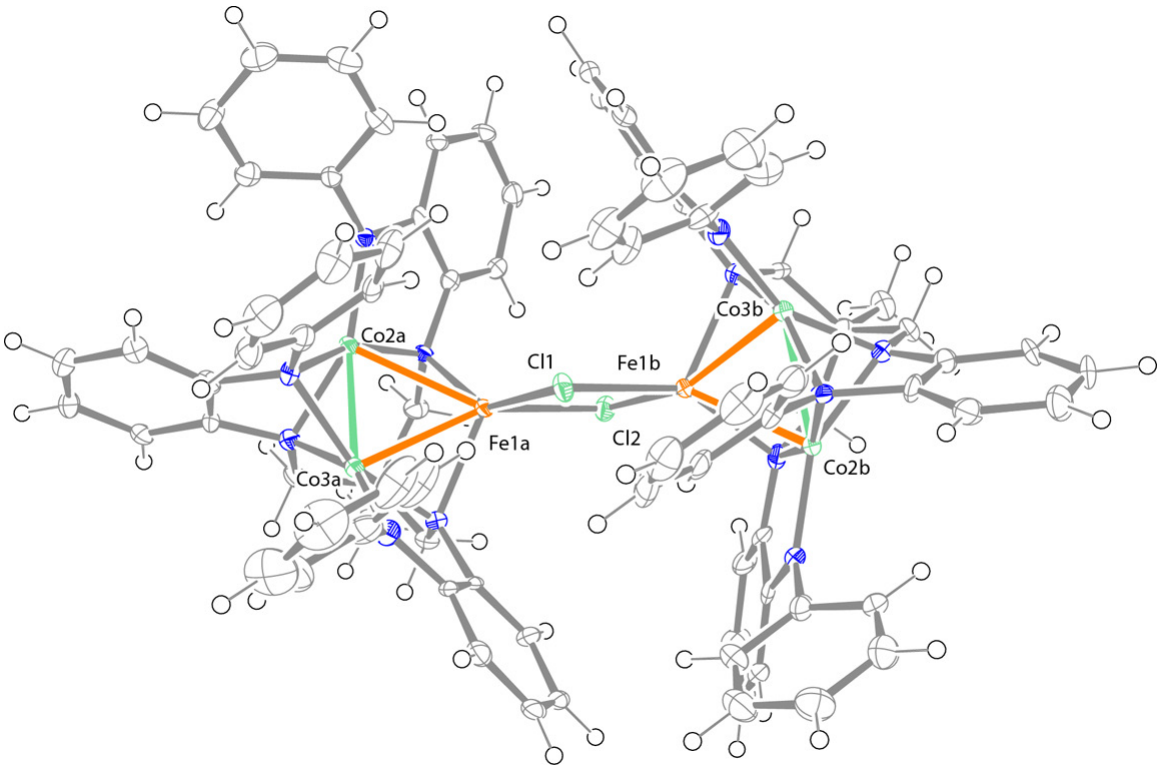

Figure S7. Zero-field ^{57}Fe Mössbauer spectrum of **2**. Simulation yields the following parameters: (blue, 28.7%) δ = 0.28 mm/s, $|\Delta E_Q|$ = 2.38 mm/s, γ = 0.23 mm/s; (green, 24.9%) δ = 0.17 mm/s, $|\Delta E_Q|$ = 2.67 mm/s, γ = 0.10 mm/s; (gold, 29.0%) δ = 0.72 mm/s, $|\Delta E_Q|$ = 1.32 mm/s, γ = 0.14 mm/s; (pink, 17.4%) δ = 1.18 mm/s, $|\Delta E_Q|$ = 2.37 mm/s, γ = 0.26 mm/s.

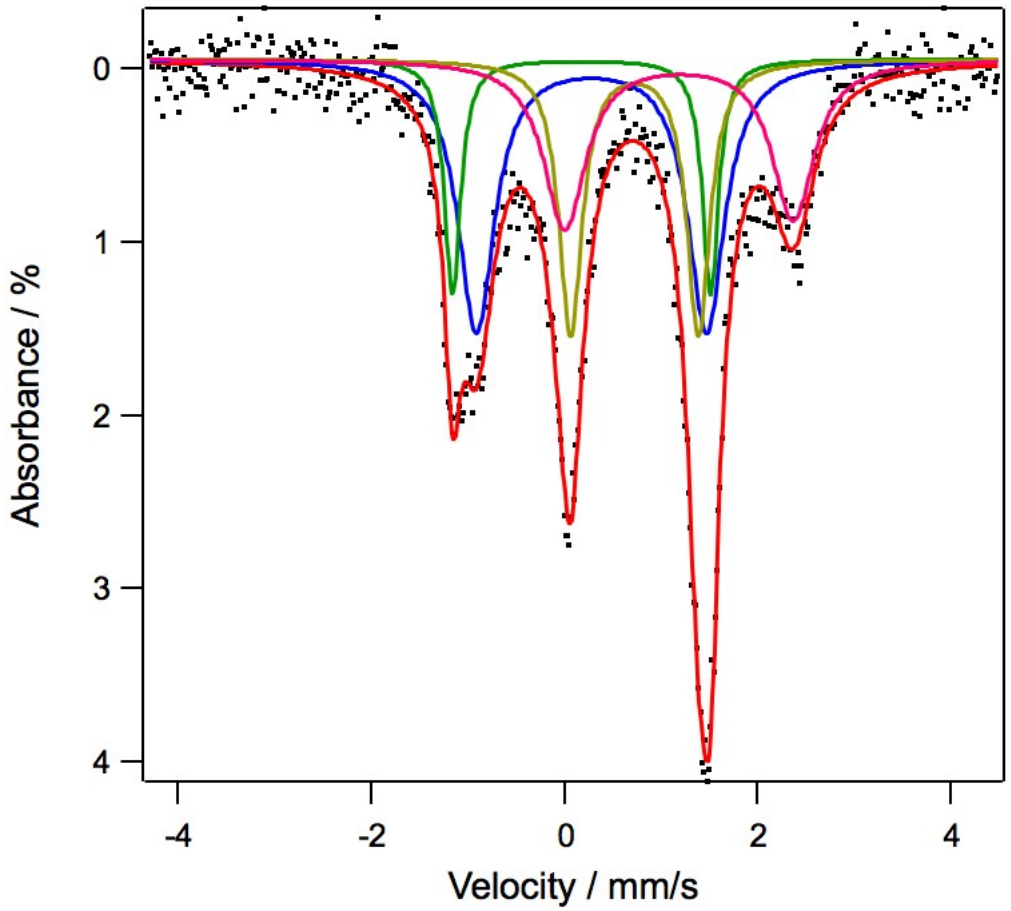

Figure S8. Zero-field ^{57}Fe Mössbauer spectrum of **3**. Simulation yields the following parameters: (blue, 38.9%) δ = 0.21 mm/s, $|\Delta E_Q|$ = 2.69 mm/s, γ = 0.18 mm/s; (green, 38.9%) δ = 0.73 mm/s, $|\Delta E_Q|$ = 1.39 mm/s, γ = 0.18 mm/s; (gold, 22.3%) δ = 1.16 mm/s, $|\Delta E_Q|$ = 2.35 mm/s, γ = 0.26 mm/s.

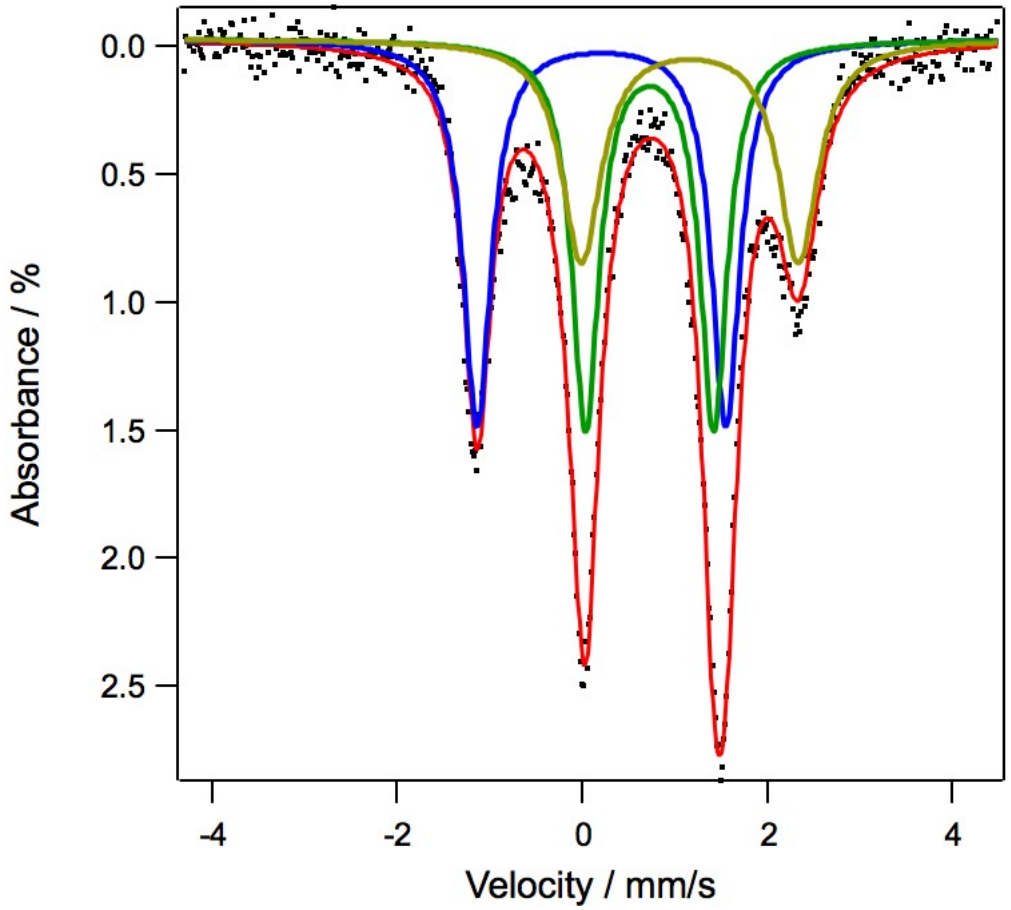

Figure S9. Zero-field ^{57}Fe Mössbauer spectrum of **4**. Simulation yields the following parameters: (blue, 56.7%) δ = 0.83 mm/s, $|\Delta E_Q|$ = 1.41 mm/s, γ = 0.26 mm/s; (green, 22.1%) δ = 0.21 mm/s, $|\Delta E_Q|$ = 2.92 mm/s, γ = 0.15 mm/s; (gold, 21.1%) δ = –0.01 mm/s, $|\Delta E_Q|$ = 2.36 mm/s, γ = 0.23 mm/s.

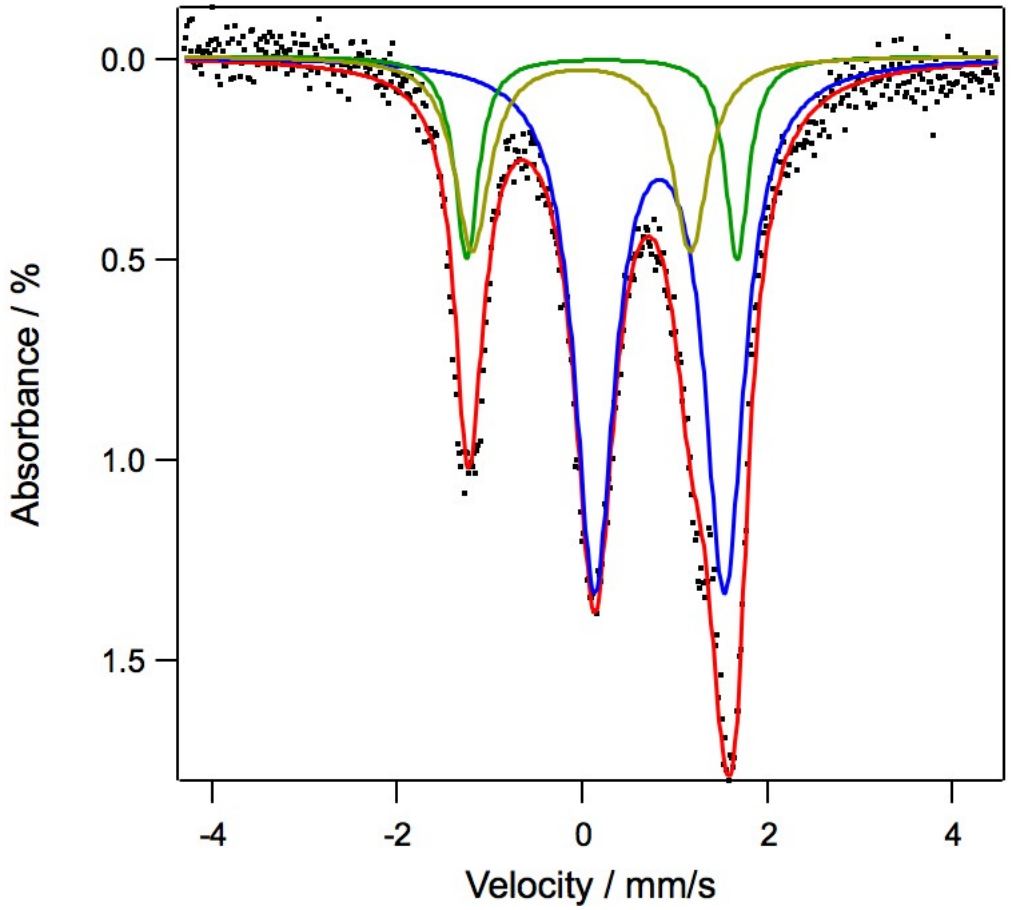

Figure S10. Zero-field ^{57}Fe Mössbauer spectrum of **5**. Simulation yields the following parameters: $\delta = 0.72$ mm/s, $|\Delta E_Q| = 1.05$ mm/s, $\gamma = 0.23$ mm/s.

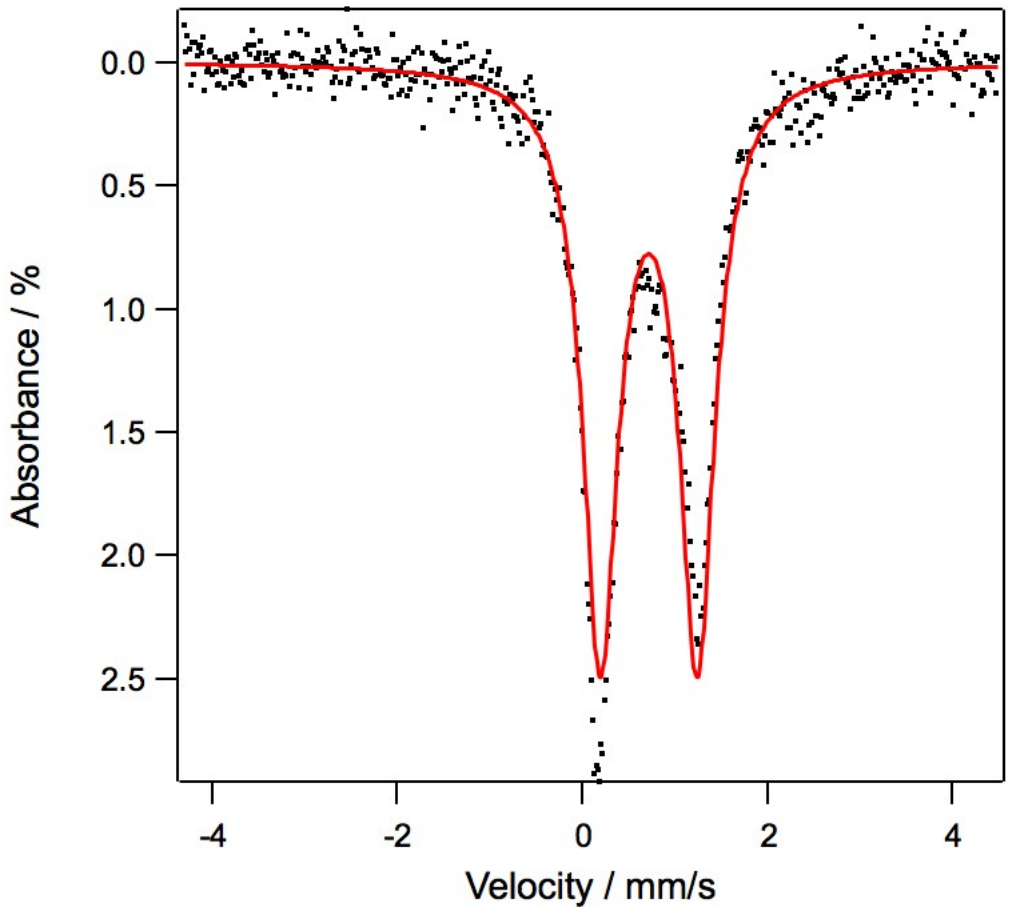

Figure S11. Zero-field ^{57}Fe Mössbauer spectrum of **6**. Simulation yields the following parameters: $\delta = 0.69$ mm/s, $|\Delta E_Q| = 1.38$ mm/s, $\gamma = 0.17$ mm/s.

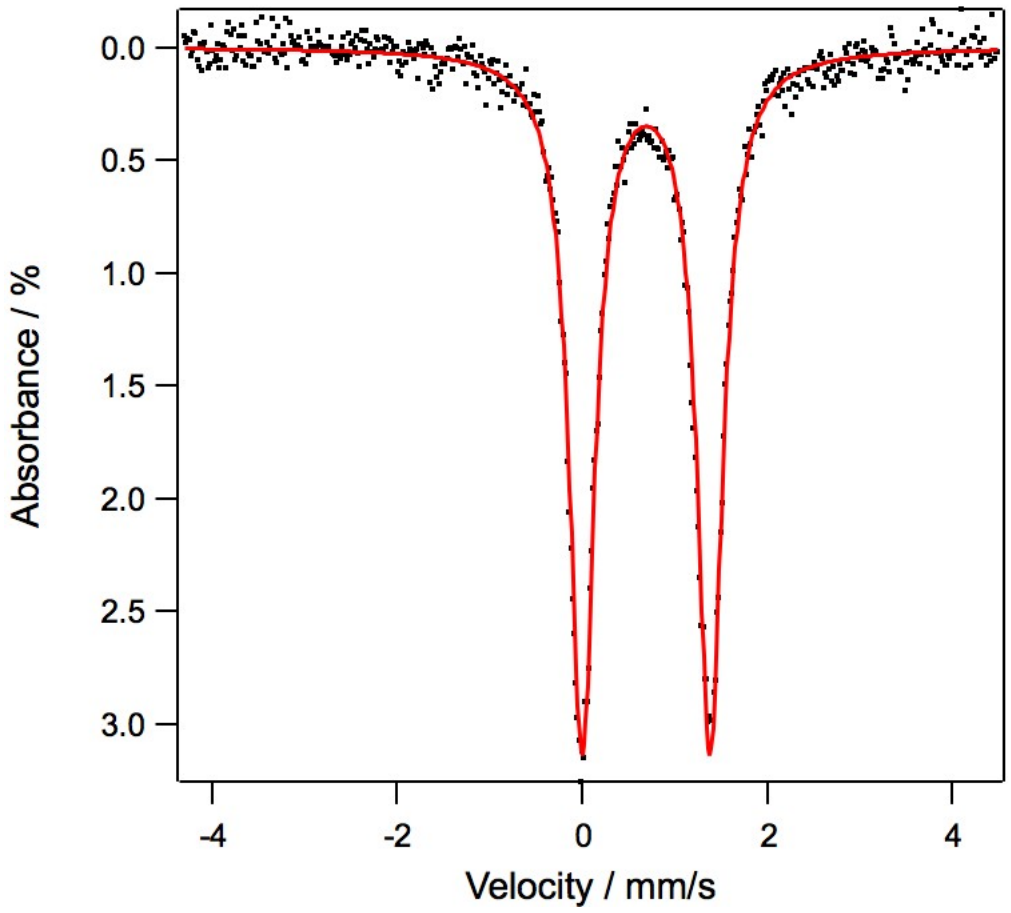

Figure S12. Zero-field ^{57}Fe Mössbauer spectrum of **7**. Simulation yields the following parameters: (blue, 33.3%) δ = 0.19 mm/s, $|\Delta E_Q|$ = 2.68 mm/s, γ = 0.12 mm/s; (green, 33.3%) δ = 0.31 mm/s, $|\Delta E_Q|$ = 2.48 mm/s, γ = 0.31 mm/s; (gold, 33.3%) δ = 0.71 mm/s, $|\Delta E_Q|$ = 1.27 mm/s, γ = 0.24 mm/s.

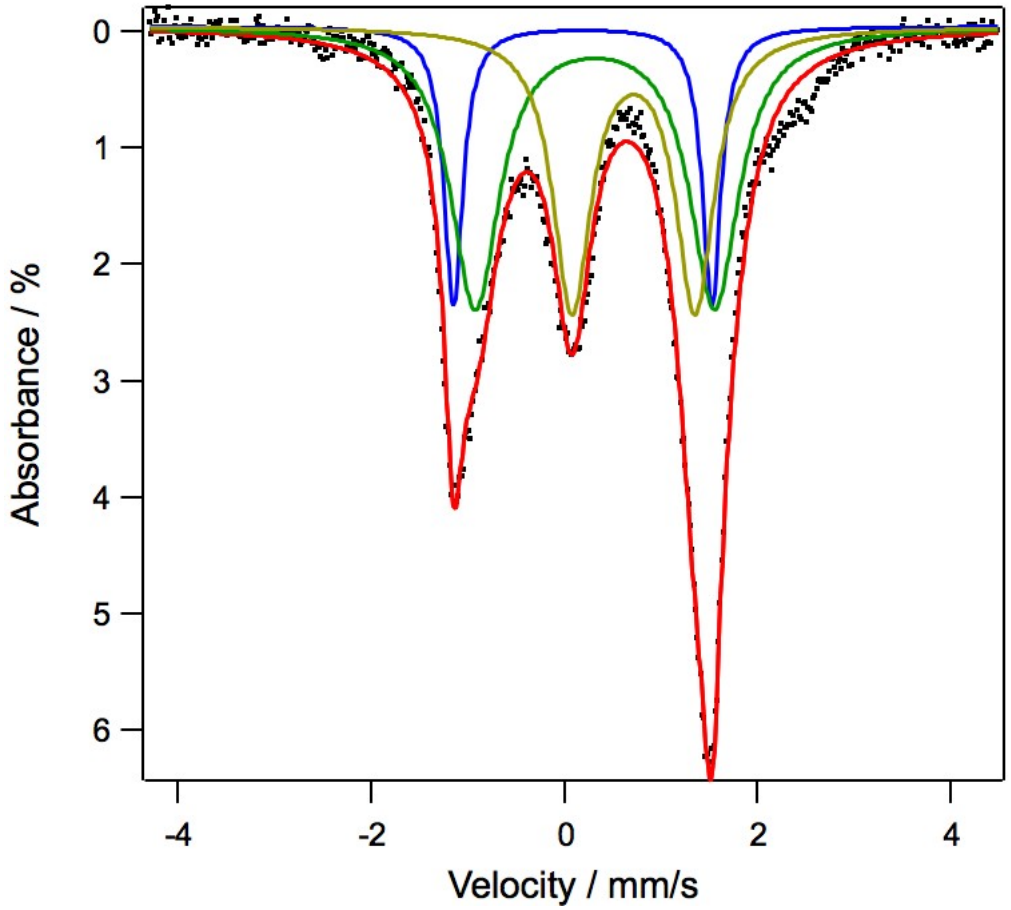

Figure S13. Calibration curve for Fe and Co quantification by X-ray fluorescence. Linear fit shown (y = 0.626x).

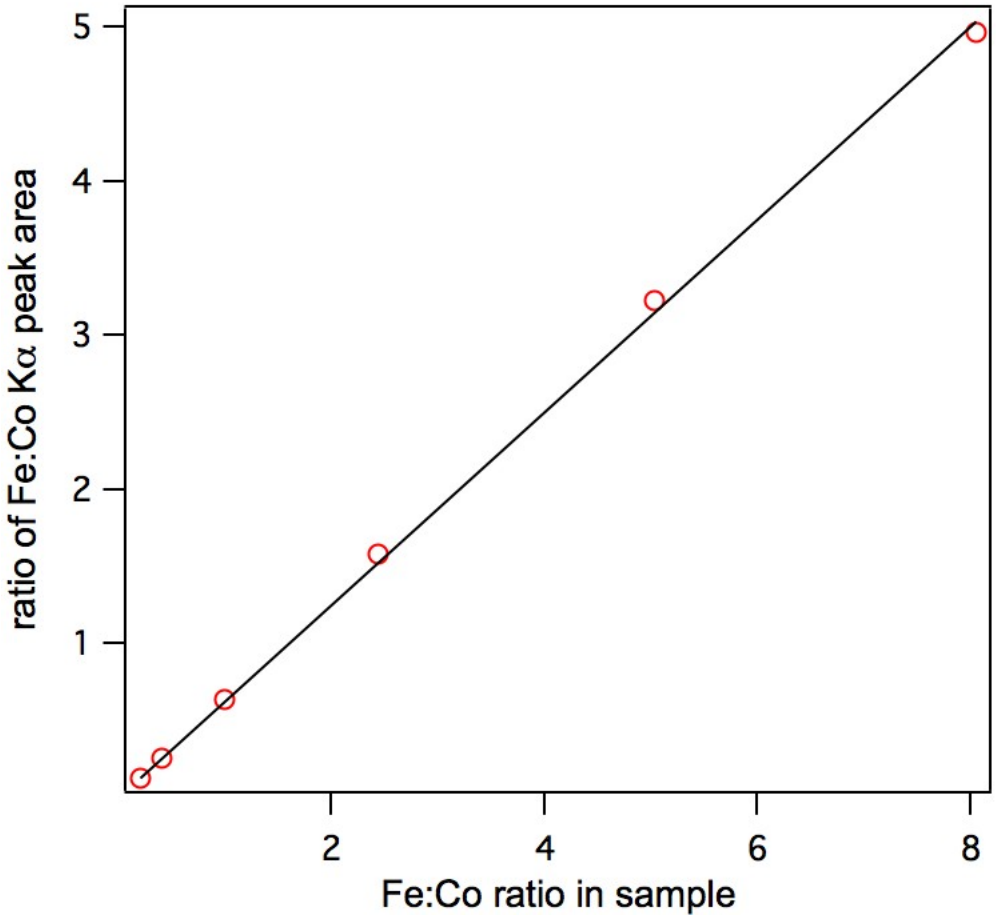

Figure S14. X-ray fluorescence spectrum of **3**. Data (black circles); fit (blue), Fe component of fit (dashed red), Co component of fit (dashed green).

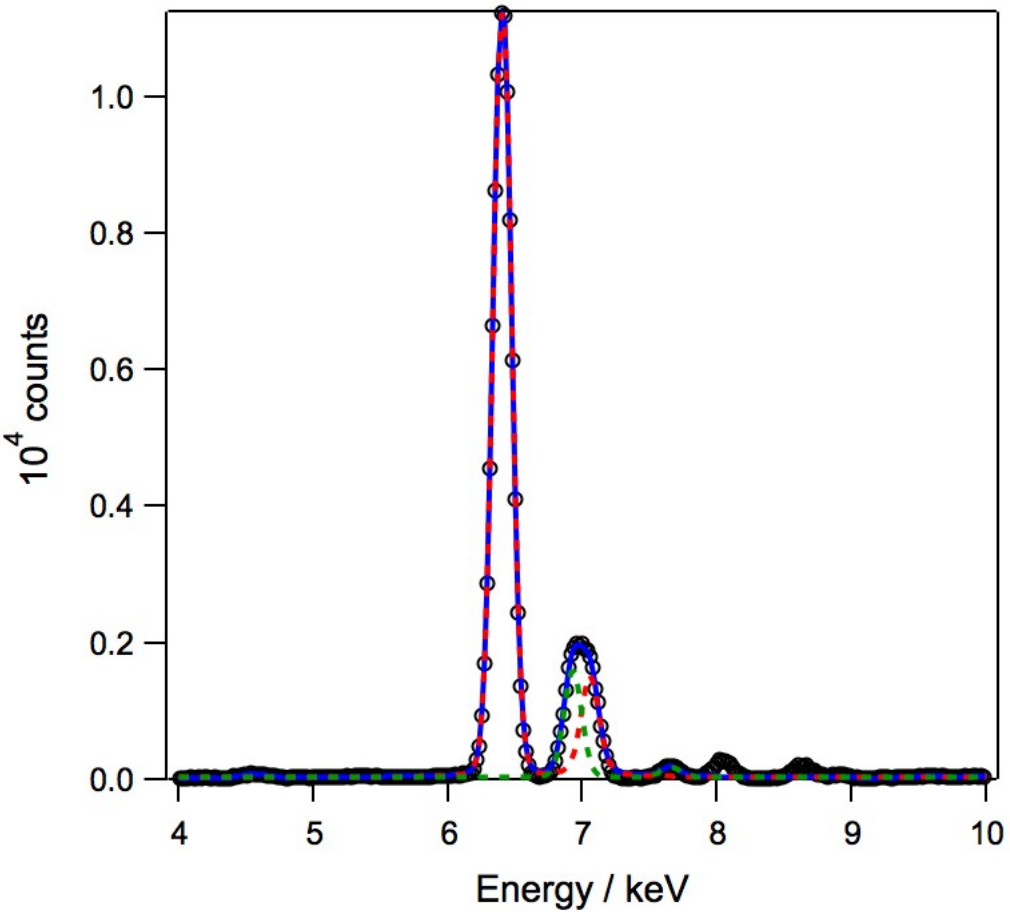

Figure S15. X-ray fluorescence spectrum of **4**. Data (black circles); fit (blue), Fe component of fit (dashed red), Co component of fit (dashed green).

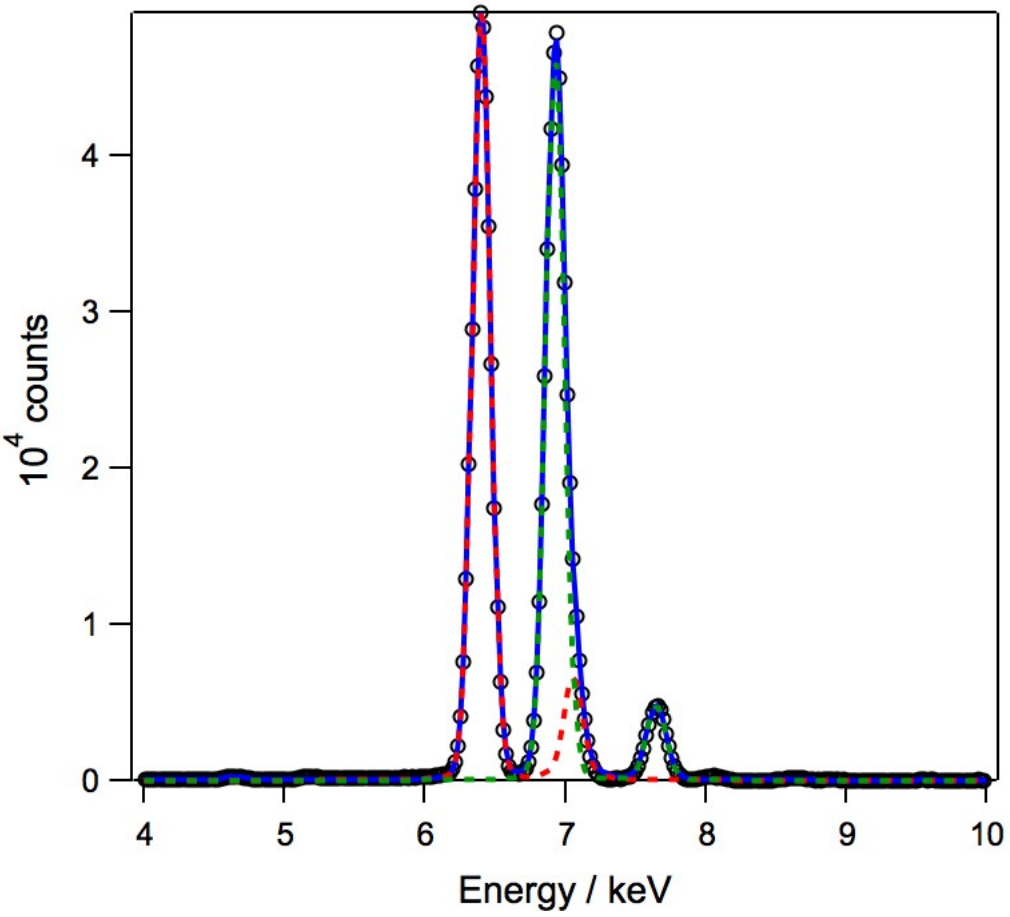

Figure S16. X-ray fluorescence spectrum of **5**. Data (black circles); fit (blue), Fe component of fit (dashed red), Co component of fit (dashed green).

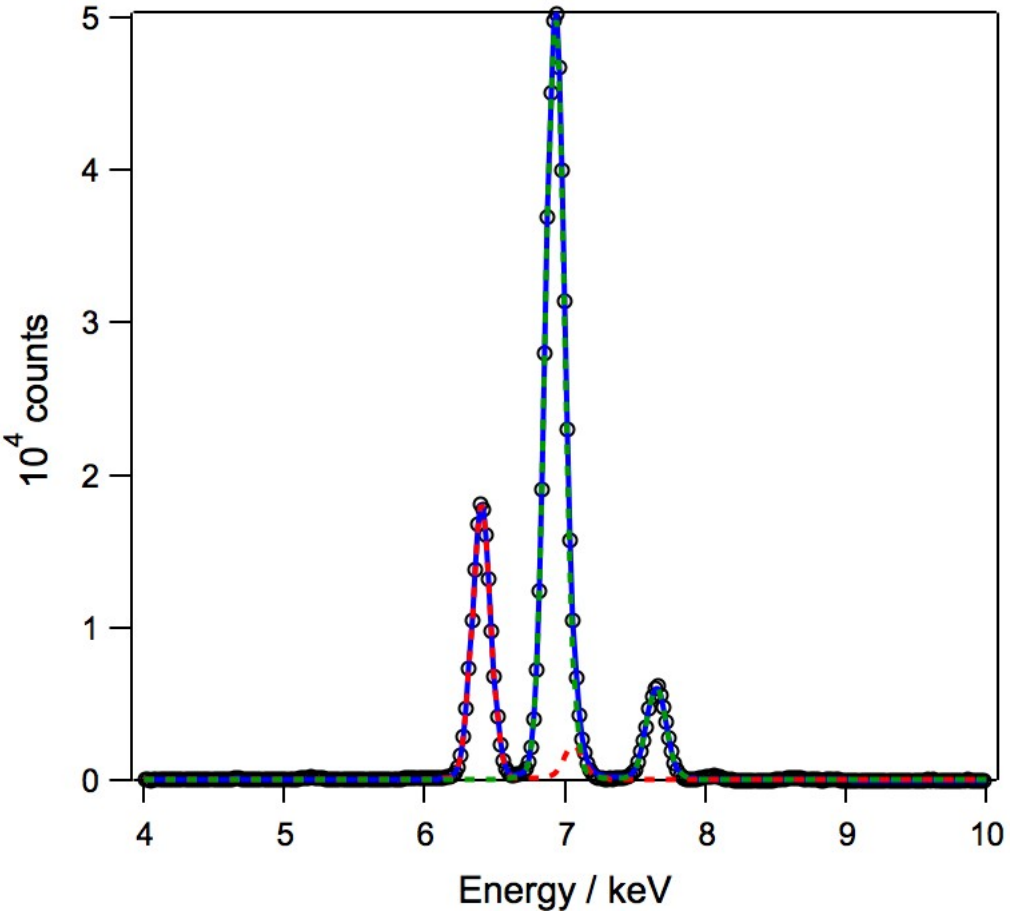

Figure S17. X-ray fluorescence spectrum of **6**. Data (black circles); fit (blue), Fe component of fit (dashed red), Co component of fit (dashed green).

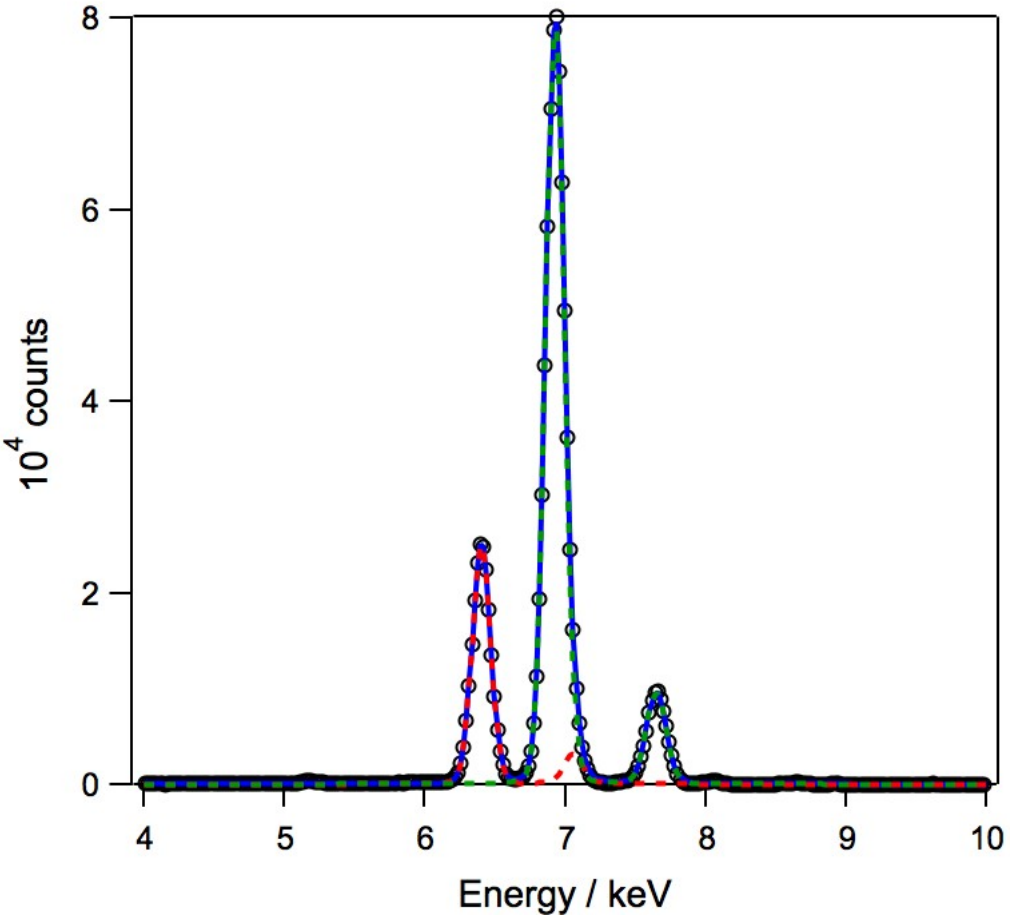

Figure S18. ^{1}H NMR data for **4** (green), **5** (blue) and **6** (red).

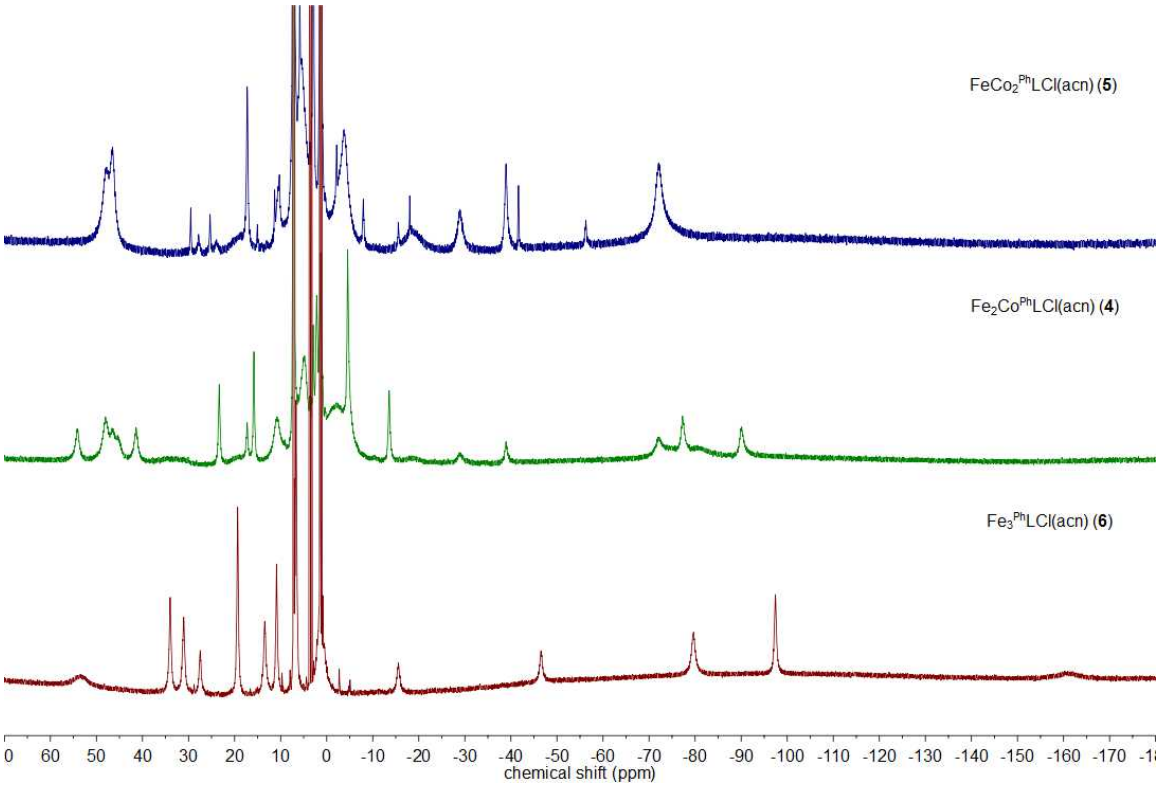

Figure S19. Variable-temperature magnetic susceptibility and reduced magnetization data for **4** with best simulation overall ($\boldsymbol{S}_1 = 2$, $\boldsymbol{S}_2 = 1$, $J = -4.25$ cm^{-1}, $D_1 = 5.25$ cm^{-1}, $D_2 = -20$ cm^{-1}, $g = 2.46$).

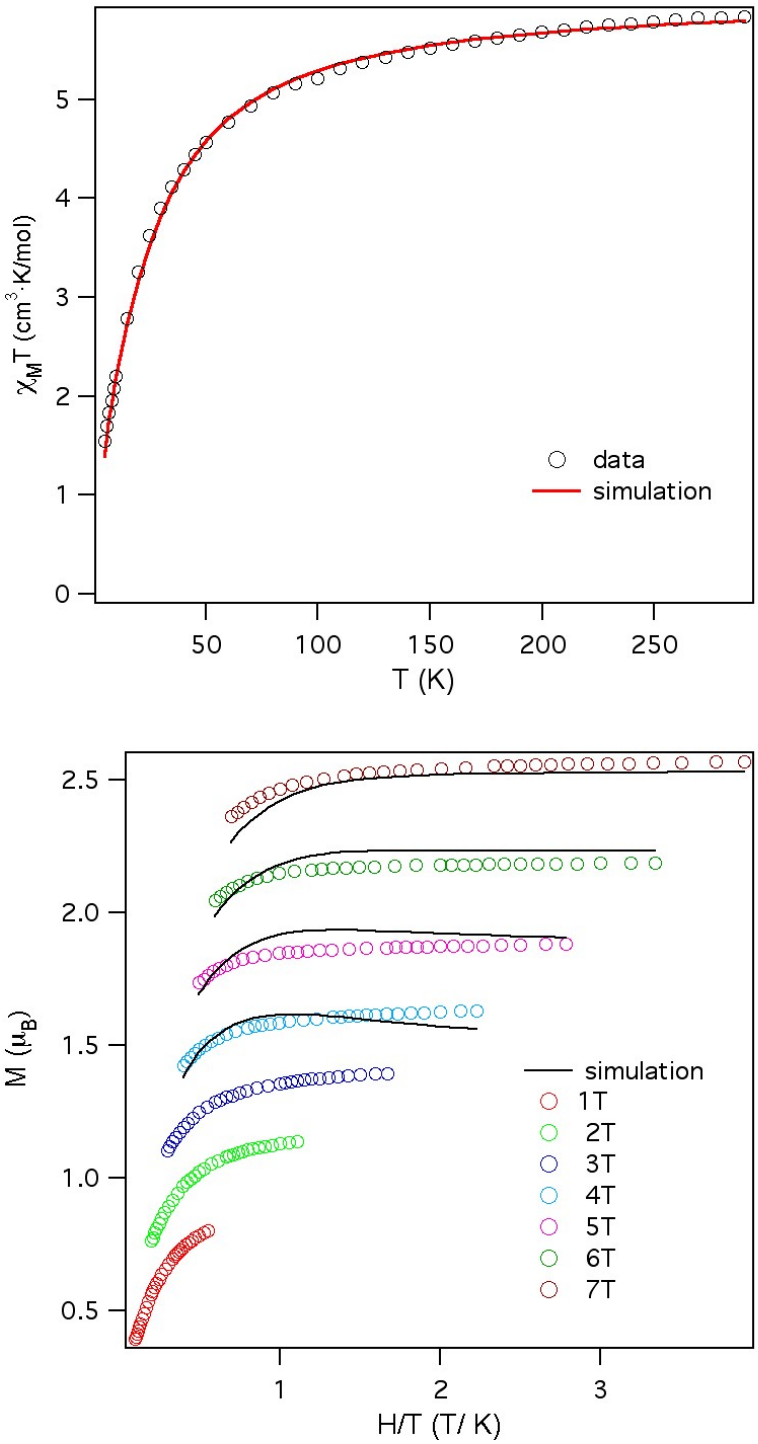

Figure S20. Variable-temperature magnetic susceptibility and reduced magnetization data for **5** with best overall simulation parameters ($\boldsymbol{S}_1 = 2$, $\boldsymbol{S}_2 = 1/2$, $J = -4.75$ cm^{-1}, $D_1 = 4.0$ cm^{-1}, $g = 2.34$).

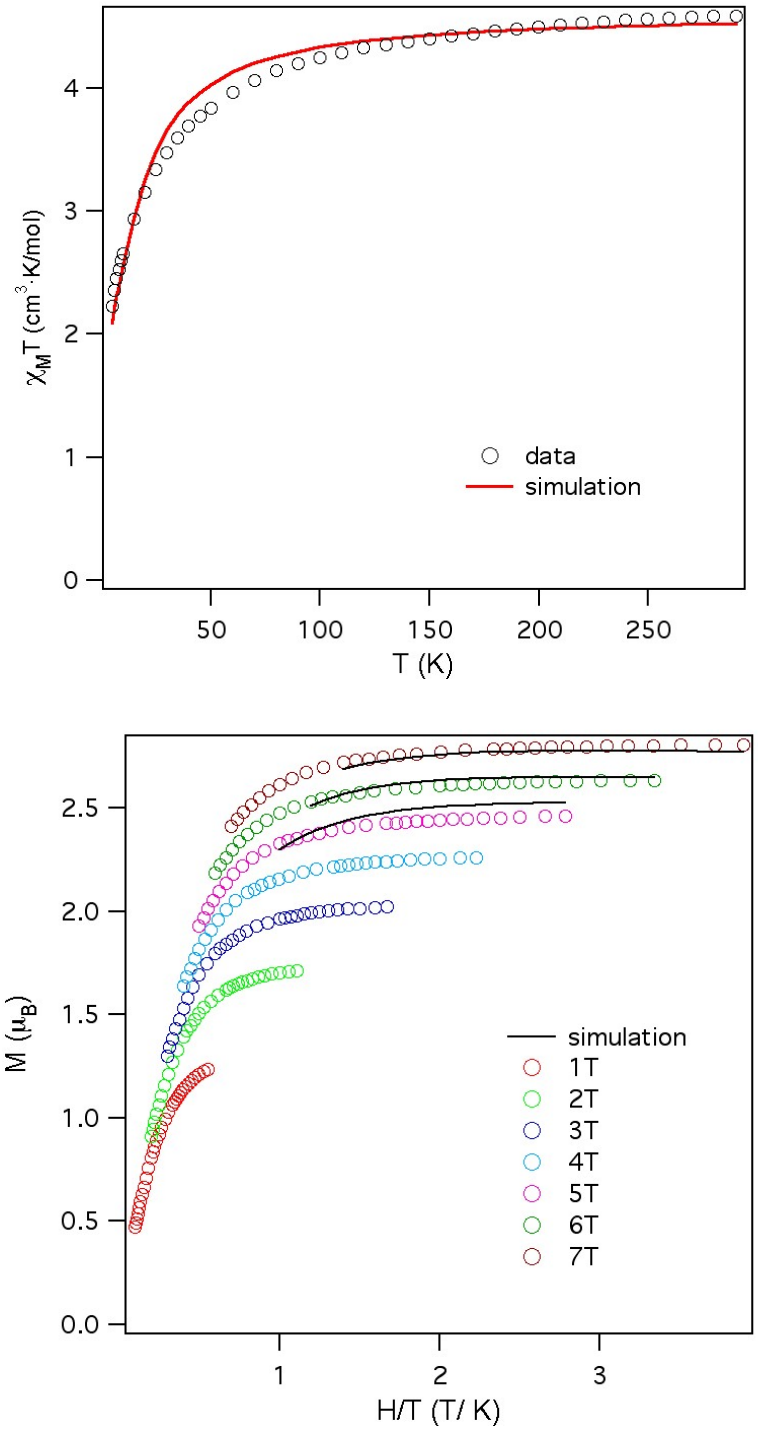

Figure S21. Zero-field ^{57}Fe Mössbauer spectrum of **2** after stirring for 30 min with 0.5 eq ^{57}Fe-enriched $FeCl_2(thf)_2$. Simulation yields the following parameters: (blue, 35.2%) δ = 0.67 mm/s, $|\Delta E_Q|$ = 1.20 mm/s, γ = 0.18 mm/s; (green, 35.2%) δ = 0.19 mm/s, $|\Delta E_Q|$ = 2.67 mm/s, γ = 0.26 mm/s; (gold, 29.5%) δ = 1.02 mm/s, $|\Delta E_Q|$ = 2.33 mm/s, γ = 0.27 mm/s.

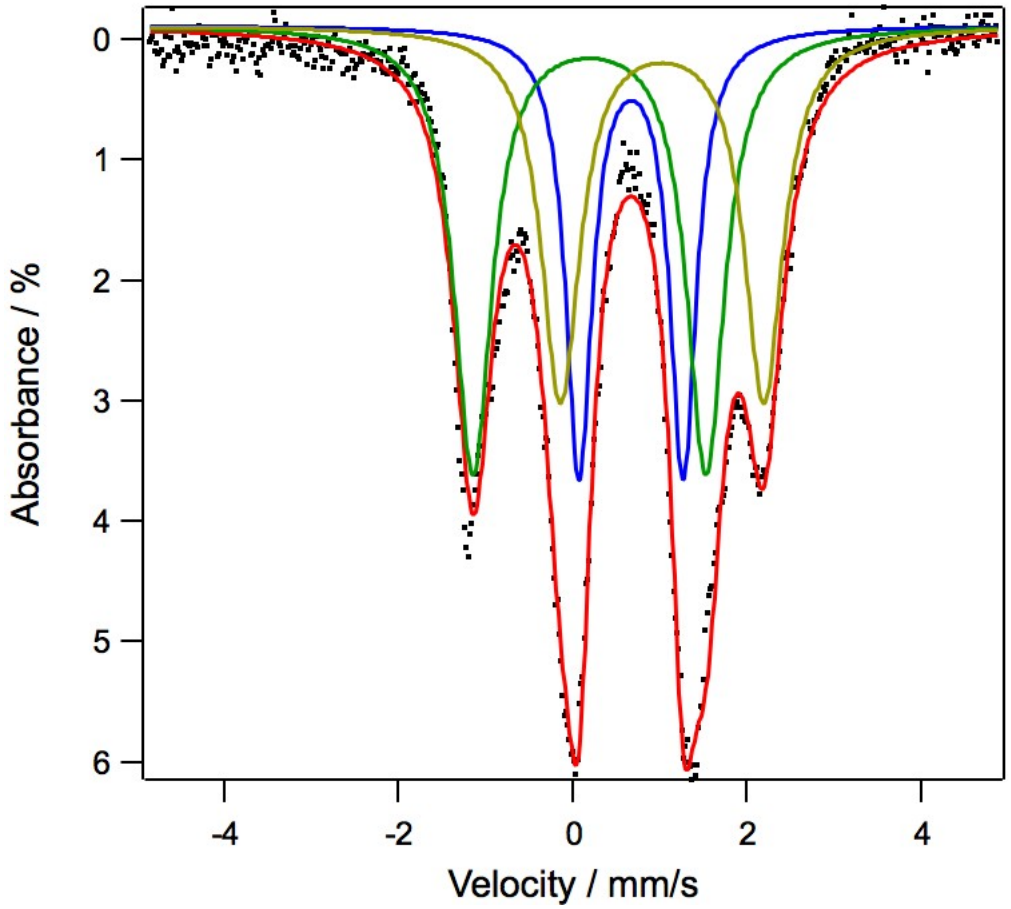

Figure S22. Zero-field ^{57}Fe Mössbauer spectrum of **2** after stirring for 2.5 h with 0.5 eq ^{57}Fe-enriched $FeCl_2(thf)_2$. Simulation yields the following parameters: (blue, 35.4%) δ = 0.58 mm/s, $|\Delta E_Q|$ = 1.40 mm/s, γ = 0.22 mm/s; (green, 35.4%) δ = 0.19 mm/s, $|\Delta E_Q|$ = 2.66 mm/s, γ = 0.29 mm/s; (gold, 29.2%) δ = 1.16 mm/s, $|\Delta E_Q|$ = 2.11 mm/s, γ = 0.26 mm/s.

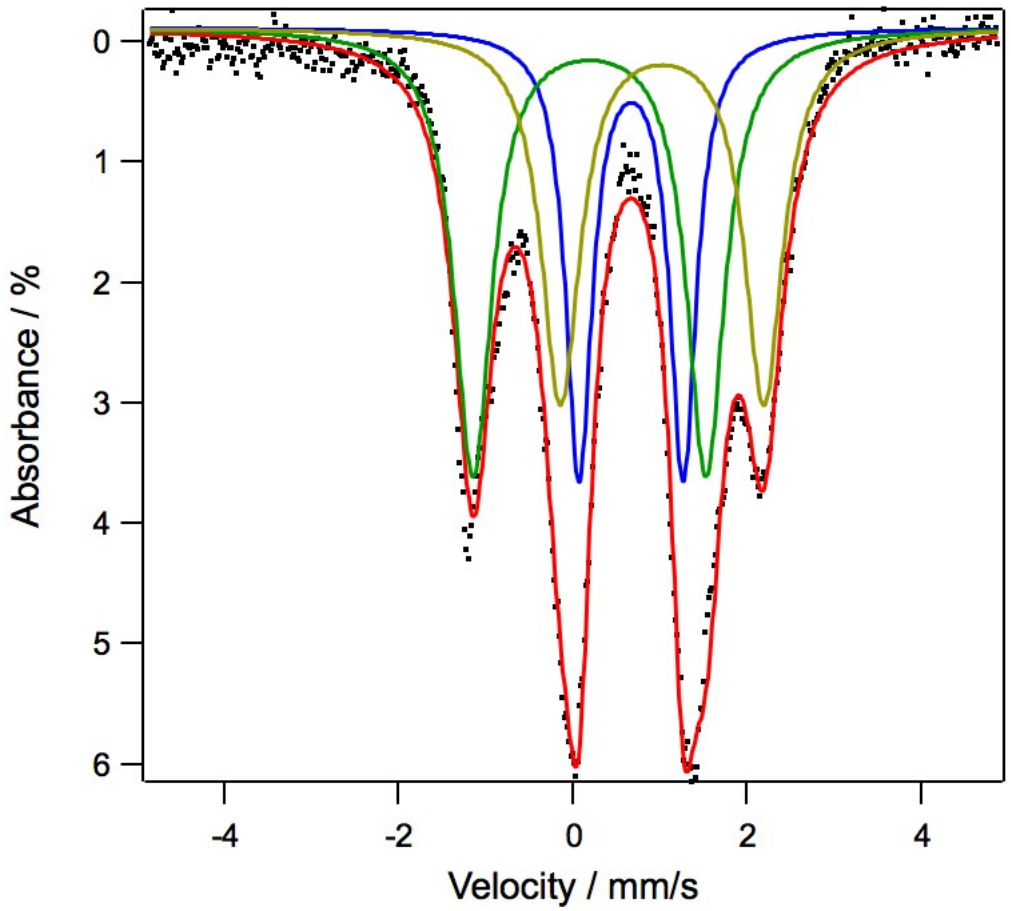

Figure S23. Zero-field ^{57}Fe Mössbauer spectrum of **2** after stirring for 15 h with 0.5 eq ^{57}Fe-enriched $FeCl_2(thf)_2$. Simulation yields the following parameters: (blue, 36.5%) δ = 0.64 mm/s, $|\Delta E_Q|$ = 1.25 mm/s, γ = 0.19 mm/s; (green, 38.8%) δ = 0.15 mm/s, $|\Delta E_Q|$ = 2.56 mm/s, γ = 0.24 mm/s; (gold, 24.7%) δ = 0.99 mm/s, $|\Delta E_Q|$ = 2.54 mm/s, γ = 0.40 mm/s.